amplitude and strong heterogeneity (Yang et al., 2022a, 2022b). Vertically, the reservoir is divided into two formations, S-B and Tanuma, with no observed edge or bottom water. The porosity ranges from 14.00% to 20.00%, and the permeability varies from 0.01 10 ^{3} to 5.00 10 ^{3} m^{2}. The formation crude oil has a viscosity of 0.451 mPa s, classifying it as a low-viscosity medium crude oil. Due to the poor reservoir quality, single-well production rates are low, production declines rapidly, and water injection remains challenging. Consequently, it is imperative to evaluate gas injection as a potential method to enhance recovery efficiency in this reservoir.

Ultra-low-permeability carbonate reservoirs are primarily developed through three approaches: depletion, waterflooding, and gas injection (Mogensen and Masalmeh, 2020; Mohammadi et al., 2022; Song and Li, 2018; Song et al., 2024a; Su and Liao, 2014; Sun et al., 2022; Wang et al., 2020; Zhang et al., 2021). In the San Andres oilfield of the United States, early depletion development yielded limited success because strong reservoir heterogeneity resulted in high residual oil saturation after primary recovery, leaving a large portion of crude oil unrecovered (Yang et al., 2017). Al-Murayri et al. (2019) conducted a laboratory feasibility study on low-salinity and polymer flooding in a low-permeability carbonate reservoir in Kuwait. The waterflooding efficiency achieved with low-salinity water reached up to 70%, and the addition of polymer further enhanced the recovery efficiency to 82%.

Water injection in ultra-low-permeability carbonate reservoirs often suffers from low imbibition efficiency, poor injectivity, and formation damage (Yu et al., 2019), thereby rendering gas injection a more favorable development approach for such reservoirs. Compared with waterflooding, gas injection can more readily establish an effective displacement pressure system, significantly reduce interfacial tension (IFT), and enhance oil swelling and viscosity reduction effects (Choubineh et al., 2019; Han et al., 2015, 2018; Hu et al., 2018; Ju et al., 2012; Liu et al., 2017; Liu and Chen, 2010; Wan and Liu, 2018; Yuan et al., 2020; Zhu et al., 2021). Gas flooding can be categorized into two types: immiscible and miscible displacement. Immiscible displacement primarily utilizes the expansion energy of injected gas to quickly establish a pressure system, displacing crude oil in the pores and increasing recovery. However, in strongly heterogeneous reservoirs, two-phase coexistence within the pore space promotes gas channeling, resulting in limited incremental recovery during area-wide displacement. In contrast, miscible flooding eliminates the phase interface entirely, reduces IFT to near zero, mobilizes crude oil trapped in small throats, and effectively delays gas channeling. Its combined effects of oil swelling and viscosity reduction substantially improve crude oil mobility and overall recovery efficiency.

Keyvani and Safaei et al. (Keyvani et al., 2024; Li et al., 2022; Safaei et al., 2021) further emphasized that the efficiency of miscible gas flooding strongly depends on achieving complete phase contact, as well as on diffusion and mass-transfer processes that govern miscibility development and displacement stability. Their findings demonstrated that molecular diffusion between injected gas and crude oil accelerates component exchange, sustains phase equilibrium, and enhances sweep efficiency in both carbonate and tight formations. These insights provide theoretical support for understanding the miscible flooding behavior discussed in this study. Similarly, Tan et al. (2022) systematically investigated the mechanisms of CO_2 enhanced oil recovery (EOR) in carbonate reservoirs and concluded that, in addition to the extraction of light components, reducing IFT, and improving oil swelling and viscosity reduction, CO_2 diffusion and mass transfer in crude oil are also key mechanisms controlling recovery performance. Liu et al. (2013) experimentally evaluated the feasibility of associated gas injection in a Middle Eastern porous carbonate reservoir and found that gas injection improved crude oil mobility through swelling and viscosity reduction, achieving a displacement efficiency of 52.02%. Likewise, Figuera et al. (2016) and Deinum et al. (Deinum et al., 2007; Al-Hadhrami et al., 2007) investigated CO_2 and hydrocarbon gas injection in the Abu oilfield and the A reservoir of the Harweel field, respectively, demonstrating that miscible gas flooding significantly enhanced crude oil mobility and increased the recovery factor by more than 20%.

Numerical and physical simulations are the primary approaches for evaluating development strategies in extra-low-permeability carbonate reservoirs. Saadawi (2010) employed numerical simulation to assess the performance of various development strategies namely, waterflooding and gas injection and different injection parameters, including injectant type and injection mode, in typical ultra-low-permeability carbonate reservoirs. They concluded that waterflooding in such reservoirs encounters major challenges, such as injection difficulties and pronounced crude oil degassing, resulting in unsatisfactory development performance. In contrast, gas injection maintains reservoir pressure, reduces viscosity, improves crude oil mobility, and enhances incremental oil recovery, increasing the recovery factor by 15% 19%. In addition, numerous researchers have conducted miscible flooding experiments on carbonate reservoirs using various injection media and methods. For example, Shi et al. (2017) investigated a low-permeability carbonate reservoir in the Middle East using NMR to examine the displacement efficiency differences under different waterflooding schemes in heterogeneous reservoir layers. They found that recovery efficiency varied significantly between layer-by-layer and simultaneous injection production modes. After waterflooding, residual oil mainly existed as oil films in large pores, while small pores were occupied by bound water. Li et al. (2020) addressed the challenges of strong heterogeneity and unreliable forecasting in large, thick carbonate reservoirs by classifying vertical stacking patterns of reservoir layers and integrating them into injection well network designs. They developed type curves for waterflooding in different stacking configurations, substantially improving prediction efficiency. Wei et al. (2022) focused on issues such as gas channeling, high gas oil ratios, and inefficient gas recycling observed during more than a decade of miscible hydrocarbon gas injection in a typical Middle Eastern low-permeability carbonate reservoir. Through numerical simulation, they proposed a comprehensive evaluation framework for miscible gas flooding performance, identified key factors influencing gas channeling, and developed optimization strategies to improve injection efficiency. Al-Hajeri et al. (Al-Hajeri et al., 2010; Salma et al., 2011), Al-Riyamy et al. (2005), and Abedini et al. (2015) combined core flooding experiments with numerical simulations to investigate enhanced oil recovery performance in low-permeability carbonate reservoirs using CO_2 and hydrocarbon gas injection. Their results indicated that these reservoirs can achieve substantial incremental recovery before gas breakthrough, with continuous gas injection maintaining high reservoir pressure and significantly prolonging the stable production period. However, despite extensive experimental and numerical research, the underlying mechanisms governing miscible gas displacement in ultra-low-permeability carbonate reservoirs remain insufficiently understood.

In summary, both field experience and numerical studies have demonstrated that gas injection represents a more effective development strategy for ultra-low-permeability carbonate reservoirs. To address the challenges identified above, this study established a high-temperature and high-pressure NMR online gas displacement and long-core flooding experimental system. Gas

flooding simulation experiments were performed to investigate the effects of different injection media and parameters on microscopic displacement behavior, recovery efficiency, and flow characteristics in ultra-low-permeability carbonate reservoirs by integrating laboratory experiments with numerical simulations. The results show that, in such tight formations, macroscopic fluid flow is dominated by non-Darcy behavior with a distinct threshold pressure gradient, while at the microscopic scale, gas diffusion from larger pores into smaller throats drives oil displacement. The coupling between molecular diffusion and the threshold pressure gradient jointly controls ultimate recovery efficiency, providing new insights into gas injection mechanisms in ultra-low-permeability carbonate reservoirs (Fig. 1).

71#1

71##1 =

Based on the PVT data of formation fluids from representative wells in the study area, the original reservoir oil was reconstituted by mixing degassed crude oil and separator gas under initial reservoir conditions (pressure: 34.45 MPa, temperature: 89 C, and gas oil ratio (GOR): 209.20 m^3/m^3), in accordance with relevant industry standards. The measured saturation pressure of the reconstituted oil sample was 24.51 MPa, with a single-stage degassed GOR of 204.63 m^3/m^3 and a viscosity of 0.458 mPa s at the saturation pressure. These parameters closely match those of the original reservoir fluids, confirming the accuracy of the reconstitution process. The compositions of the reconstituted reservoir crude oil and the injected gases are summarized in Table 1.

The hydrocarbon gas used for injection was formulated based on the PVT report (Table 1), whereas N_2 and CO_2 were commercial-grade gases with a purity of 99.00%. Before conducting long-core and NMR displacement experiments, gas injection expansion tests and slim-tube tests were carried out to systematically evaluate the effects of gas injection on the high-pressure physical properties of formation fluids and to determine the miscibility between the injected gases and crude oil. The results of the gas injection expansion tests (Table 2) show that as the injected gas volume increased, the elastic expansion capacity of the crude oil improved while its viscosity decreased, demonstrating a clear enhancement of fluid mobility. Under reservoir conditions (pressure: 34.45 MPa, temperature: 89 C), the minimum miscibility pressures (MMPs) obtained from the slim-tube tests were 45.00 MPa for N_2, 30.20 MPa for CO_2, and 31.20 MPa for hydrocarbon gas (Fig. 2). Therefore, under the current reservoir conditions, N_2 injection corresponds to immiscible flooding, whereas CO_2 and hydrocarbon gas injections achieve miscible flooding.

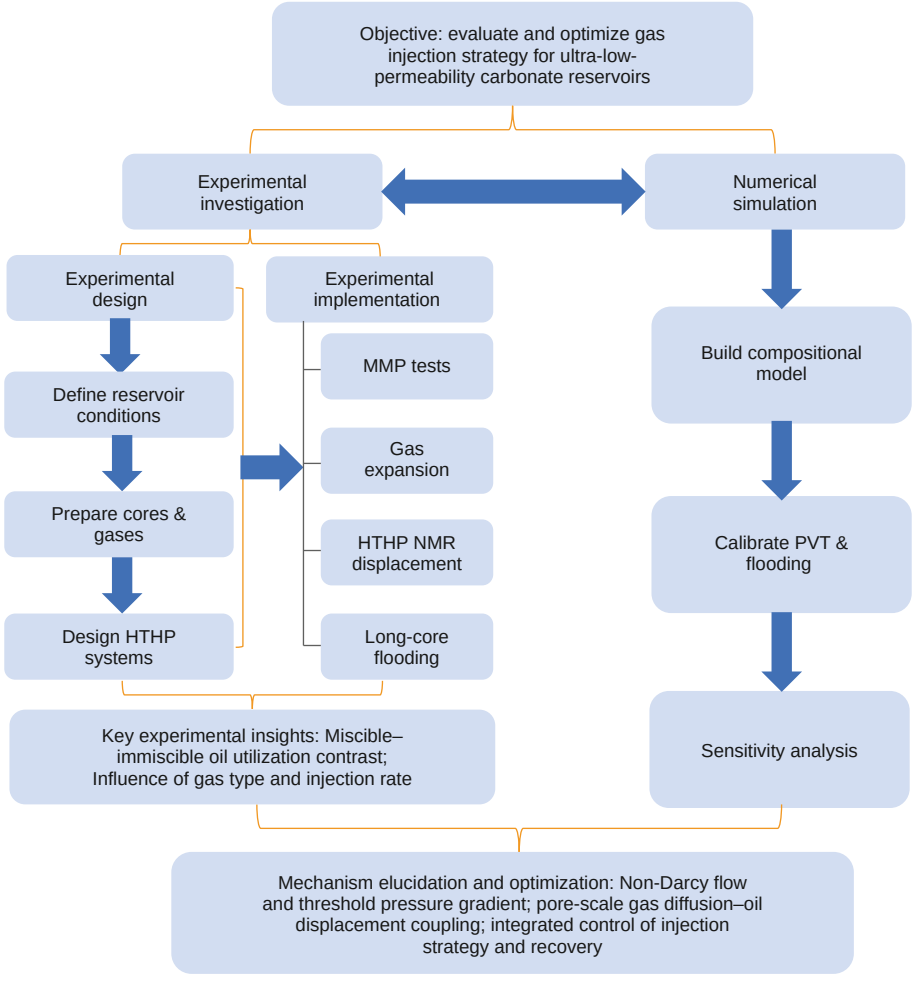

Research workflow illustrating the experimental design, implementation, and numerical simulation processes used to investigate gas flooding mechanisms and optimize injection strategies in ultra-low-permeability carbonate reservoirs.

Composition of blended reservoir crude oil and injected gases.

Components	Molar fraction of formation crude oil components, %	Molar composition of the injected hydrocarbon gas, %
CO_2	0.49	2.83
N_2	0.11	0.01
C_1	37.18	64.62
C_2	11.56	16.57
C_3	9.64	14.02
C_4	1.39	0.60
C_4	1.64	0.59
C_5	2.07	0.54
C_5	1.99	0.10
C_6	5.96	0.12
C_{7+}	27.97	/

Results of gas injection expansion tests.

Injection medium	Molar fraction of gas injection, %	GOR, m^3/m^3	Saturation pressure, MPa	Volume coefficient	Expansion coefficient	Density, g/cm^3	Viscosity, cP
/	0.00	205.20	24.55	1.5993	1.0000	0.6944	0.458
N_2	4.44	220.02	27.17	1.6450	1.0258	0.6903	0.449
	9.09	238.50	32.14	1.6863	1.0531	0.6874	0.442
	14.01	260.26	36.62	1.7347	1.0809	0.6825	0.436
	19.29	286.52	42.17	1.8010	1.1065	0.6767	0.427
	24.55	316.34	46.90	1.8480	1.1368	0.6731	0.421
CO_2	5.37	223.60	25.52	1.6554	1.0356	0.6881	0.447
	9.76	241.34	26.48	1.7397	1.0686	0.6825	0.435
	14.89	264.41	27.45	1.8030	1.1122	0.6782	0.428
	20.07	290.68	28.97	1.8688	1.1452	0.6717	0.413
	25.00	319.08	30.48	1.9271	1.1954	0.6667	0.402
Hydrocarbon gas	4.66	222.45	26.14	1.6469	1.0254	0.6895	0.449
	9.08	240.13	27.59	1.7154	1.0556	0.6855	0.440
	15.38	268.53	29.72	1.7788	1.0910	0.6793	0.431
	20.61	295.52	32.48	1.8424	1.1293	0.6732	0.420
	25.43	323.74	35.93	1.8922	1.1703	0.6682	0.412

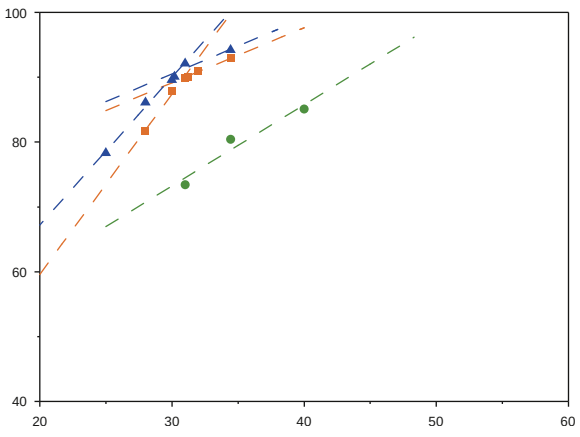

Relationship between oil displacement efficiency and pressure in slim-tube experiments for different injection media.

The injection water was formulated based on the water quality analysis of produced water from the field. It is classified as $CaCl_2$-type formation water with a total salinity of 220,104 mg/L and a pH of 6.30. The mass concentrations of the major cations are Ca^{2+} (16,685 mg/L), Mg^{2+} (3189 mg/L), Sr^{2+} (690 mg/L), K^{+} (900 mg/L), and Na^{+} (61,500 mg/L), while the anions include Cl (136,898 mg/L), HCO_3 (15 mg/L), and SO_4^{2} (227 mg/L). To eliminate interference from formation water signals during the NMR oil displacement experiments, the injection water was prepared using heavy water (D_2O) as the solvent.

71#171!

For the NMR online oil displacement experiments, a core sample from the S-B3 formation was used, measuring 4.70 cm in length and 2.51 cm in diameter, with a permeability of 0.40 10 ^{3} m^2 and a porosity of 10.00%. To better represent the in-situ reservoir characteristics in the long-core flooding experiments, multiple short plug cores were assembled into a composite long core using the harmonic averaging method to determine the overall permeability. Filter papers were inserted between core segments to minimize capillary end effects (Wang et al., 2022). The final composite core measured 24.27 cm in total length, with an average porosity of 15.20% and an average permeability of 0.30 10 ^{3} m^2 (Table 3).

71712 / / 82 259 >? &

71#11

To investigate the distribution and behavior of crude oil in the pores under miscible and immiscible flooding conditions, a high-pressure and high-temperature (HPHT) online NMR gas flooding system was developed. The system consists of an injection pump unit, intermediate container, NMR core holder, back-pressure regulator, differential pressure transducer, temperature control system, and gas flowmeter (Fig. 3). A Ruska automatic displacement pump was employed to ensure precise flow control, with a speed accuracy of 0.001 mL/min. The temperature control system maintains stability within 0.1 C, while the gas flowmeter provides a measurement accuracy of 0.1 mL. The magnetic field strength of the NMR scanner is 0.30 0.05 T, ensuring stable and reliable signal acquisition under HPHT conditions.

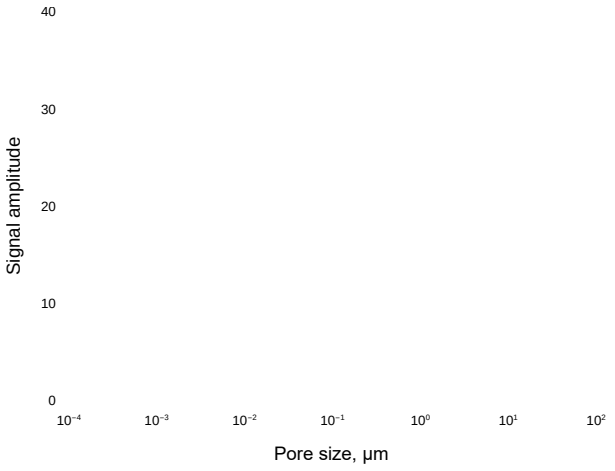

(a) Fluid distribution profile map for immiscible N_2 flooding

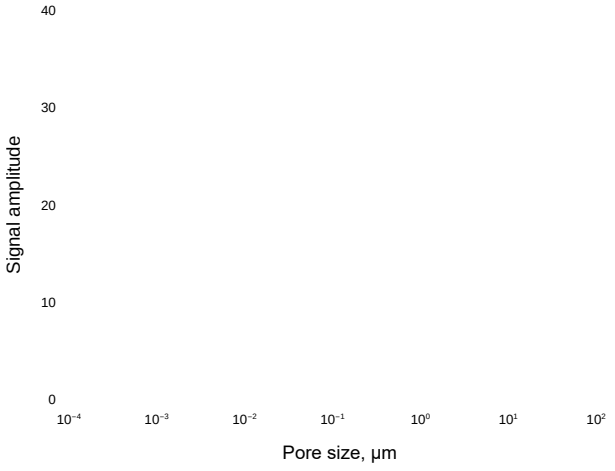

(b) Fluid distribution profile map for miscible CO_2 flooding

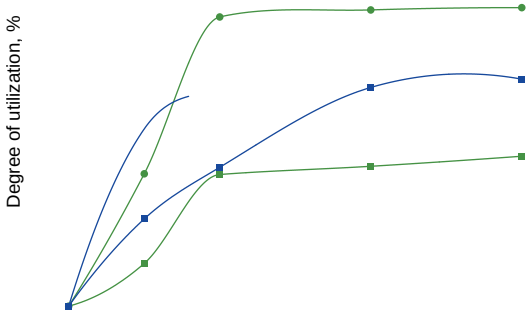

(c) Displacement efficiency of oil under N_2 and CO_2 flooding

Fluid distribution and recovery state before and after gas injection displacement.

(4.50 m). However, neither N_2 nor CO_2 significantly mobilized oil in micro-pores (0.0 7 m) (Fig. 5(a) and (b)).

For large pores (4.50 m), CO_2 miscible and N_2 immiscible flooding yielded comparable mobilization efficiencies of 69.95% and 76.81%, respectively. However, in the early displacement stage (0.4 HCPV), N_2 flooding achieved a higher efficiency of 74.39%, exceeding CO_2 flooding by 18.54% (Fig. 5(c)). This difference is attributed to the high solubility of CO_2 (Table 2), which leads to extensive dissolution into crude oil during the early phase. This dissolution reduces the amount of free CO_2 available for direct displacement, thereby weakening its sweeping effect in large pores. Consequently, N_2 flooding exhibits superior early-stage displacement efficiency in the macropore network.

For small pores (0.07 4.50 m), CO_2 miscible flooding achieved an oil mobilization efficiency of 58.39%, nearly 20.00% higher than that of N_2 flooding. However, during the initial stage, both gases exhibited comparable performance (Fig. 5(c)), as early gas dissolution mainly occurred in large pores and had limited influence on smaller ones. With continued injection, CO_2''s high solubility and miscible displacement mechanism facilitated substantial dissolution into small-pore oil, enhancing elastic expansion and ultimately improving oil mobilization.

Overall, these results demonstrate that miscible flooding significantly enhances oil mobilization within small pores and substantially improves the overall displacement efficiency compared to immiscible flooding.

! "

A comparison of the experimental results from Schemes 1 3 demonstrates that the type of injection medium has a pronounced effect on the overall oil displacement efficiency. Under continuous gas injection at 34.45 MPa and an injection rate of 0.1250 mL/min, the gas breakthrough volumes for N_2, CO_2, and hydrocarbon gas were 0.5, 0.7, and 0.7 HCPV, respectively. The corresponding total displacement efficiencies were 47.28%, 75.52%, and 71.37%. The primary displacement stage occurred prior to gas breakthrough (Fig. 6).

Analysis indicates that both CO_2 and hydrocarbon gas achieved miscible flooding, resulting in delayed breakthrough compared with N_2 immiscible flooding. The prolonged main displacement stage under miscible conditions substantially improved overall recovery efficiency. In addition, the stronger swelling and viscosity reduction effects of CO_2 (Table 2) yielded a 4.15% higher displacement efficiency relative to hydrocarbon gas. These results clearly demonstrate that, for ultra-low-permeability carbonate reservoirs, miscible flooding with CO_2 or hydrocarbon gas significantly outperforms N_2 immiscible flooding, with CO_2 showing

$ Comparison of oil displacement efficiencies using different injection media under continuous gas injection.

slightly superior performance. However, considering field implementation feasibility, gas availability, and economic practicality, hydrocarbon gas is recommended as the preferred injection medium for reservoir development.

#

! "

%#11 & * & & B& &

%#11#1 & * & & B& &

A comparison of Schemes 3, 4, and 5 highlights the influence of injection pressure on displacement performance during continuous hydrocarbon gas flooding. At injection pressures of 34.45, 31.00, and 27.00 MPa, the gas breakthrough volumes progressively decreased from 0.8 HCPV to 0.7 and 0.6 HCPV, respectively. The corresponding displacement efficiencies were 54.89%, 57.72%, and 50.03%, while the total recovery efficiencies declined from 72.28% to 66.27% and 52.47%, respectively. These results indicate that earlier gas injection timing, corresponding to higher reservoir pressures, significantly enhances oil recovery (Fig. 7).

Mechanistically, earlier gas injection ensures that the reservoir pressure remains above the minimum miscibility pressure (MMP) of hydrocarbon gas (31.20 MPa), thereby promoting miscible flooding and improving displacement effectiveness. Under such conditions, higher injection pressure enhances gas solubility in crude oil, leading to increased oil swelling, viscosity reduction, and improved fluid mobility, which collectively delay gas breakthrough. Furthermore, elevated injection pressures improve gas injectivity by enhancing compressibility and pore-scale expansion effects, which lower overall flow resistance and facilitate the displacement of resident liquid from the pore space. Consequently, these synergistic effects yield higher recovery factors at elevated pressures. The experimental results confirm that natural depletion results in poor recovery, whereas gas injection above the MMP achieves markedly superior performance. Overall, miscible flooding significantly outperforms immiscible flooding, demonstrating a clear dependence of recovery efficiency on injection pressure and miscibility conditions.

%#1171 & * & & B& &

The preceding section demonstrated that earlier gas injection timing enhances flooding performance. Accordingly, Schemes 6 and 7 were designed with injection initiated at 34.45 MPa and pressure maintained at 100% of the initial reservoir pressure. A comparison among Schemes 6, 3, and 7 conducted under the same reservoir pressure (34.45 MPa) but at different injection rates (0.0625, 0.1250, and 0.2500 mL/min) showed that the gas breakthrough volumes advanced from 0.8 HCPV to 0.7 HCPV as the rate increased. The corresponding displacement efficiencies were 54.89%, 54.81%, and 59.91%, while the total recovery efficiencies decreased sequentially from 72.28% to 71.37% and 70.44%. These results indicate that overall flooding efficiency tends to decline with increasing injection rate (Fig. 8).

Mechanistically, the behavior of miscible gas flooding in ultra-low-permeability reservoirs differs from that observed in conventional formations. Although higher injection rates are often associated with improved sweep efficiency in traditional miscible flooding, ultra-tight reservoirs rely on multiple-contact miscibility (MCM) between the injected gas and crude oil. At elevated injection rates, the reduced gas oil contact time limits interphase mass transfer, hindering the establishment of full miscibility and thereby diminishing flooding performance. Conversely, excessively low injection rates may lead to insufficient pressure maintenance, failing to overcome the threshold pressure gradient characteristic of such tight formations. Therefore, an optimal gas injection rate exists that balances pressure support and mass-transfer efficiency, ensuring the best miscible flooding performance in ultra-low-permeability carbonate reservoirs.

%#11,1 & * & & B& &

A comparative analysis was conducted between continuous gas injection (Scheme 4) and pulse gas injection (Scheme 8) under conditions where pressure decreased from 34.45 MPa to 31.00 MPa. In the pulse injection method, 0.1 pore volume (PV) of hydrocarbon gas was injected sequentially. After each injection, the inlet was closed to stabilize pressure, and the outlet was reopened to release gas until the system pressure returned to 31.00 MPa. Under these conditions, the oil displacement efficiency increased from 64.07% to 68.97%, with a delayed gas breakthrough observed for the pulse injection mode (Fig. 9). This improvement is attributed to the extended contact time between hydrocarbon gas and crude oil during pulse injection, which enhances interphase mass transfer, promotes more complete extraction, mitigates gas fingering, delays gas channeling, and ultimately improves recovery efficiency.

A similar comparison was performed for N_2 injection, involving continuous flooding (Scheme 1) and huff-and-puff injection

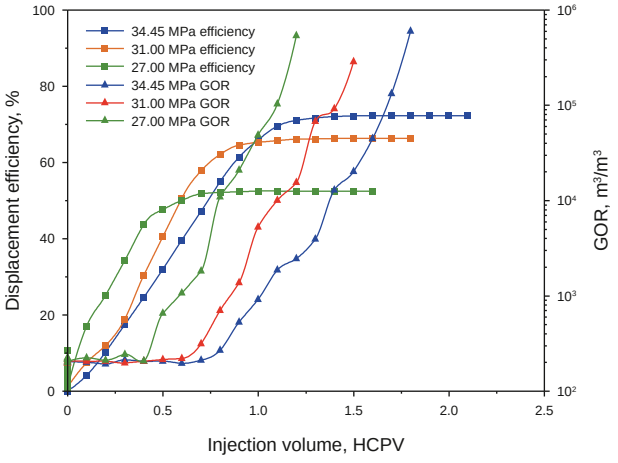

% Relationship between injected gas volume, oil recovery efficiency, and gas oil ratio (GOR) for different injection timings of hydrocarbon gas.

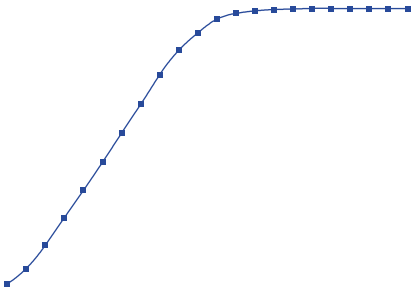

& Relationship between injected gas volume, oil recovery efficiency, and gas oil ratio (GOR) for different injection rates of hydrocarbon gas.

Saturation pressure fitting from gas injection expansion tests.

Oil expansion coefficient fitting from gas injection expansion tests.

Sensitivity analysis results for different gas injection timings.

%17171* &

At a constant reservoir pressure of 34.45 MPa, the peak recovery efficiencies for N_2, CO_2, and hydrocarbon gas were observed at injection rates of 0.0500 mL/min (48.56%), 0.0625 mL/min (76.04%), and 0.0700 mL/min (73.02%), respectively (Fig. 15). Deviations from these optimal rates led to a decline in displacement efficiency, confirming the existence of rate-dependent optimization for ultra-low-permeability reservoirs. In miscible flooding, slower injection rates promote gas oil mass transfer but reduce pressure maintenance, whereas faster rates maintain pressure but limit contact time. For immiscible N_2 flooding, optimizing the balance between gas dissolution and pressure support is essential to maximize recovery.

In the S reservoir, miscible flooding (CO_2 or hydrocarbon gas) proceeds through a multiple-contact miscibility (MCM) process, whereby the injected gas gradually extracts heavier oil components or enriches the oil with light components from the gas until phase equilibrium is achieved (Song et al., 2024b). As gas injection continues, gas molecules diffuse from larger pores into smaller throats, promoting interphase mixing and mass transfer (Tan et al., 2022). In miscible displacement, molecular diffusion between gas and oil eventually reaches equilibrium, while in immiscible N_2 flooding, diffusion-driven mass transfer still enhances crude oil mobility through partial equilibrium mechanisms. However, injection rate optimization involves a critical trade-off: Lower rates extend gas oil contact time, improving mass transfer but reducing average formation pressure, thereby limiting the ability to overcome the threshold pressure gradient; Higher rates maintain formation pressure but shorten contact time, constraining diffusion and reducing recovery.

The interplay between molecular diffusion and the threshold pressure gradient ultimately controls the overall recovery efficiency in the S reservoir. These mechanisms explain the distinct recovery trends observed in miscible (hydrocarbon gas) and immiscible (N_2) flooding (Figs. 16 and 17). Hydrocarbon gas miscible flooding achieved recovery efficiencies exceeding 60%, while N_2 immiscible flooding attained approximately 40%. Higher levels of pressure maintenance correlate positively with displacement efficiency, as gas injection simultaneously overcomes the threshold pressure gradient and enhances gas oil mass transfer. The optimal injection rates, ensuring a balance between pressure support and diffusion effectiveness, were determined to be 0.0700 mL/min for hydrocarbon gas and 0.0500 mL/min for N_2.

Sensitivity analysis results for injection rates

%171,1* & / &

To further validate the rationality of the optimized injection rate and recovery performance, sensitivity analyses were conducted for N_2, CO_2, and hydrocarbon gas at their respective